DIGITAL IMAGE PROCESSING FOR THE RECTIFICATION OF TELEVISION CAMERA DISTORTIONS*

Thomas C. Rindfleisch

Jet Propulsion Laboratory
Pasadena, California 91103

ABSTRACT

All television systems introduce distortions into the imagery they record which influence the results of quantitative photometric and geometric measurements. Digital computer techniques provide a powerful approach to the calibration and rectification of these systematic effects. Non-linear as well as linear problems can be attacked with flexibility and precision. Methods which have been developed and applied for the removal of structured system noises and the correction of photometric, geometric, and resolution distortions in vidicon systems are briefly described. Examples are given of results derived primarily from the Mariner Mars 1969 television experiment.

Introduction

As all physically realizable instruments influence the data they collect, television cameras leave their signatures on the imagery they record. Scientific analyses of television photographs must be performed with the knowledge that the scene is observed through the camera's eye and any distortions introduced by the camera system processes potentially affect the results. The subject of this paper is the application of digital computer techniques to quantify and correct for video data distortions so that measurements and interpretations of the imagery can be based upon information as representative of the object scene as possible. This aspect of image processing represents but one of the several broad areas of application of digital methods to imagery, including camera system diagnostics, subjective detail enhancement, quantitative data rectification, and information extraction.

* This paper presents the results of one phase of research conducted at the Jet Propulsion Laboratory, California Institute of Technology, under contract number NAS 7-100, sponsored by the National Aeronautics and Space Administration.

The specific goal of the work to be discussed is the rectification of raw camera output data, using calibrated camera system performance characteristics, to produce photometrically and geometrically precise, high resolution imagery of the object scene. In approaching this problem, five major topics will be discussed including:

1. Encoding image information for the computer
2. Optimization of the system signal-to-noise properties
3. Calibration and correction of photometric distortions
4. Calibration and correction of geometric distortions
5. Calibration and restoration of image resolution

These classes of distortions are common to all camera systems, even though the physical mechanisms involved and the severity of particular types of distortion vary from sensor type to sensor type. Examples will be shown primarily illustrating the correction of distortions in vidicon television systems such as have flown on the Ranger, Surveyor, and Mariner spacecraft missions. All of this work was performed in the Image Processing Laboratory at the Jet Propulsion Laboratory using a general purpose computer, a specialized software system, and a high resolution film recorder and scanner.

Image Quantization

By their very natures, object scenes are continuous distributions of light intensities and digital computers are devices which manipulate discrete numbers. Two quantization processes are involved in converting a continuous image into an array of numbers on which the computer can perform various operations, each of which can cause serious artifacts in the processing results. The first quantization step is the two-dimensional spatial sampling of the image and the second is the binary encoding of each intensity sample. Because the major video distortions are introduced prior to the quantization procedure and because any distortions introduced in the quantization process itself are not reversible, it is important to observe certain criteria in encoding images for computer processing.

The vertical sampling of the image is generally the result of the line scanning of a raster and the horizontal sampling, the result of a subsequent periodic measurement of the one-dimensional scanned video signal. The effective density of these samples, in the image plane being scanned, must be high enough to satisfy the Nyquist sampling criterion, i.e., the sampling frequency in each direction must be at least twice the spatial frequency bandwidth in that direction. Physically this means that there must be at least two samples in a characteristic horizontal and vertical diameter of the system point spread function. This criterion guarantees that the discrete set of samples accurately describe the continuous image intensity distribution, even at points lying between the sample points. If this criterion is not satisfied (the data are aliased), then the actual behavior of the continuous image function between two sample points can deviate significantly from an interpolated estimate between those points and introduce spurious results in various geometric correction and enhancement filtering processes.

The binary encoding of each sampled intensity introduces an uncertainty in the quantized data which is related to the size of the intensity steps between encoding levels. In order to guarantee that the quantized image data are limited in their precision by the random noises of the image formation and camera sensor, a sufficient number of bits must be used to make the quantization noise insignificant. For a linear encoding to n bits of a signal such as the output of a vidicon camera with limited dynamic range V, the steps between encoding levels δV are

$$\delta V = V/2^n$$

The root-mean-square (rms) noise introduced by this encoding, σ_q, is

$$\sigma_q = \delta V/2\sqrt{3}$$

If the rms random noise at the output of the camera system is σ_r, a reasonable criterion for the number of bits required for the encoding is derived from requiring the quantization noise to be on the order of half the random noise

$$\sigma_q \lesssim \frac{1}{2}\sigma_r$$

The required number of bits is then

$$n \gtrsim \log_2\left(\frac{V}{\sigma_r}\right) - 0.8$$

If the quantization noise dominates the random noise, the possibility of processing artifacts again arises. As the quantization interval becomes comparable to the image intensity fluctuations over a local area, the quantization noise becomes highly correlated with the signal. This appears as blocks of neighboring sample points having the same encoded intensity value, thereby introducing series of plateaus or contours in the encoded data. These correlated noises cause artifacts in enhancement filtering processes in addition to limiting measurement accuracy.

System Noise

The practical limit to all quantitative or photointerpretive measurements on a properly encoded image is the presence of noise. Enhancement processes such as to improve image resolution can sharpen features only at the expense of overall signal-to-noise ratio. For these reasons, one of the most important initial steps in digital image processing is the suppression of noise so that subsequent enhancement and restoration processing can be performed on maximum signal-to-noise ratio imagery to achieve optimized results.

Many noise sources exist in imaging systems ranging from random, wideband shot and thermal noises to highly structured periodic noises. Furthermore, in situations such as space photography, it is generally not possible to obtain multiple imagery in order to use frame averaging techniques. The precise separation of any noise from the composite video of a single frame must be based on one or more quantifiable characteristics of the noise signal of interest which distinguish it uniquely from the other video components. In most real situations one has only statistical information about the various components of the total video signal and thus, even in the theoretical limit, their separation is approximate. This is certainly the case in the data output of spacecraft video systems where the dominant signal represents a complex natural scene. The essence of video noise removal is to isolate and remove the various identifiable and characterizable noise components as rigorously as possible so as to do a minimum of damage to the actual video data. In most cases, the errors introduced to the real signal by the removal process, while small, vary from point to point and are impossible to measure meaningfully since very little is known in detail about the scene being photographed and the efficacy of removal is data dependent. In the following, the removal of three different types of structured noise will be described, including periodic, long-line, and spike noises.

Periodic Noise Removal - In electronic video systems, a common noise problem arises from the coupling of periodic signals related to the raster scan and data sampling drives into the low signal portions of the video handling electronics.

These noises are generally introduced when the video scene is represented by a one-dimensional temporal signal. Because of the periodicity of this type of noise, a useful method for characterizing it is in terms of a Fourier decomposition. A one-dimensional digital power spectrum of a test scene photographed by a Mariner Mars 1969 camera is shown in Figure 1. The power spectrum clearly shows a smoothly varying background decreasing in amplitude with increasing frequency and representing the true video spectrum on which is superimposed a number of narrow, abnormally large spikes. These spikes are the various components of the periodic noises present in the Mariner system and are related to multiples of the 2400 Hertz spacecraft power supply frequency.

For well designed systems, these periodic noises exhibit phase coherence over times long compared to the frame time of the camera. For this reason, when the two-dimensional image is reconstructed, the periodic noise appears as a two-dimensional pattern exhibiting periodicity not only along the scan lines, but perpendicular to them as well. If one computes a two-dimensional Fourier transform of a reconstructed picture, as shown in Figure 2, this two-dimensional structure becomes evident. Again the actual video signal spectrum appears as a noisy continuum falling off in amplitude toward high spatial frequencies and the noise components appear as well-defined two-dimensional spikes.

Because the noise as well as the scene exhibit two-dimensional correlation, a more precise removal can be achieved by filtering the noise from the two-dimensional Fourier space than from the one-dimensional space. This can be seen by considering the effects of one-dimensional filtering as observed in the two-dimensional transform space. Since the removal of a one-dimensional frequency component is

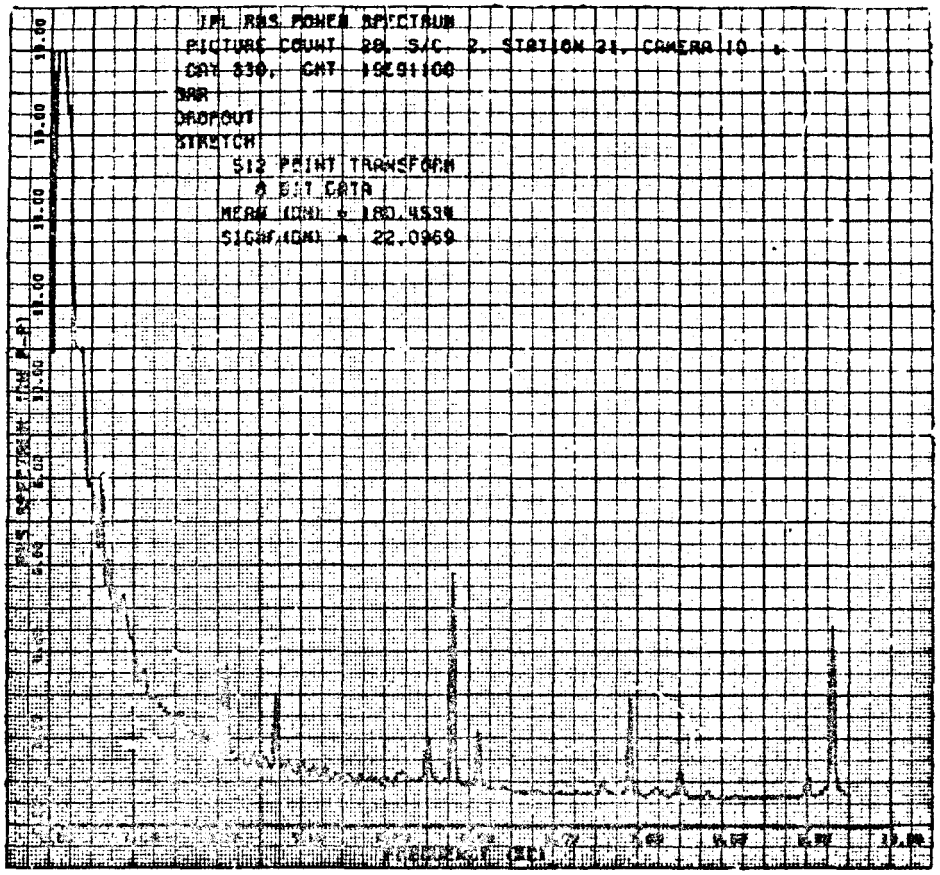

Figure 1.-Digitally computed Fourier power spectrum of test scene photographed by a Mariner Mars 1969 camera. The spectrum was computed from the one-dimensional scan output of the camera.

done irrespective of its vertical variation, the corresponding spectral components removed in two-dimensional frequency space lie in a vertical bar. Thus, since the noise component is contained in one spike along the bar, a large amount of video signal is unnecessarily removed.

Removing the two-dimensional spikes, one achieves a first order clean-up of the periodic noise components. By this method only the portion of the component spectral spikes can be isolated which protrude above the video spectrum continuum, without unduly removing the video signal. As can be seen in the power spectrum of Figure 1, the spikes clearly have skirts extending below the continuum. These skirts represent a subtle local modulation (generally amplitude modulation) of the basic noise pattern as might occur with amplitude dependence or saturation

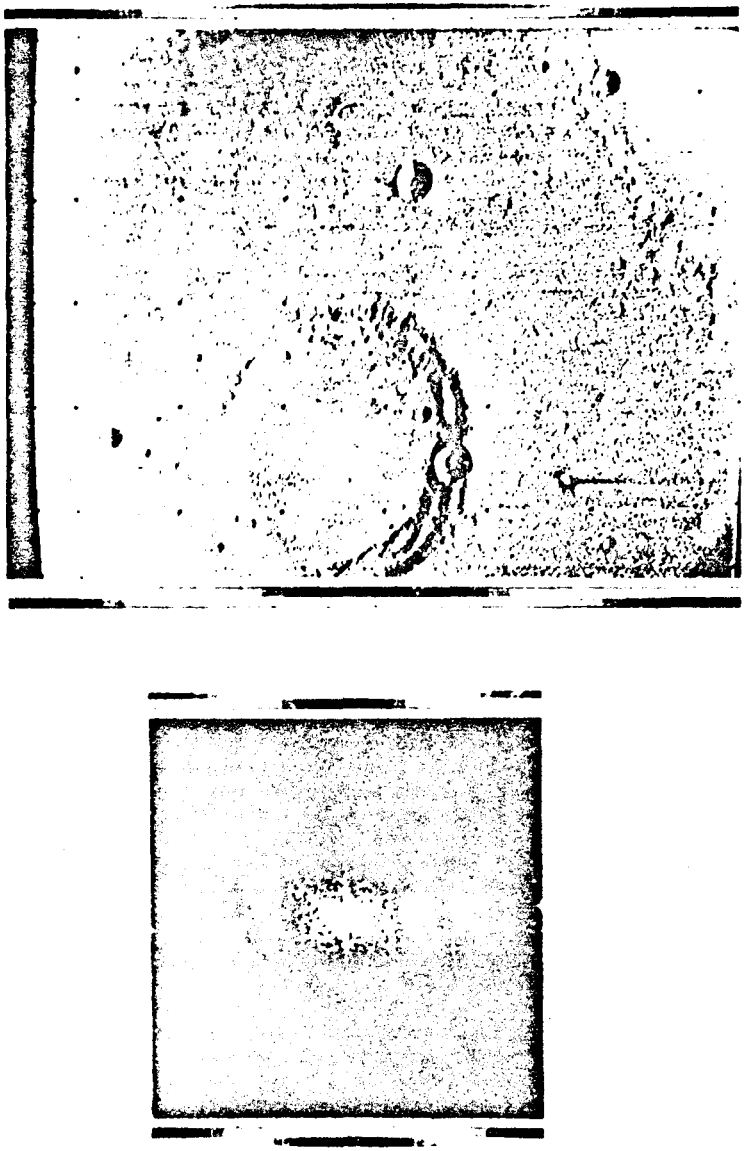

Figure 2. - The top picture is a raw photograph of Mars returned by a Mariner VI camera. Note the diagonal bands of periodic noise. The bottom picture is a digitally computed two-dimension Fourier spectrum of a portion of the top picture. The absolute spectrum amplitudes are displayed as gray levels increasing from black to white. The DC point of the spectrum is in the center of the bottom picture. Positive and negative horizontal spatial frequencies are above and below.

effects on the noise signal. These cannot be readily isolated by frequency space filtering. A more effective approach is to determine a local modulation coefficient for the idealized noise pattern derived from careful two-dimensional filtering. This coefficient is typically slowly varying relative to the resolution limits of the camera. The criterion which has been used for determining the local modulation coefficient is to minimize the variance of the noisy signal minus a variable fraction of the idealized noise pattern over a local region. If N_{ij} is the noisy image, n_{ij} is the idealized noise pattern, a_{ij} is the local modulation coefficient, and σ^2_{ij} is the "cleaned-up" signal variance for the local region of dimension M, the definition of local signal variance

$$\sigma^2_{ij} = \frac{1}{(M+1)^2} \sum_{k=-M/2}^{M/2} \sum_{l=-M/2}^{M/2} \left[(N_{i+k,j+l} - a_{ij} n_{i+k,j+l}) - (\langle N \rangle_{ij} - a_{ij} \langle n \rangle_{ij}) \right]^2$$

is used. The bracketted terms are average values defined for any matrix m_{ij} to be

$$\langle m \rangle_{ij} = \frac{1}{(M+1)^2} \sum_{k=-M/2}^{M/2} \sum_{l=-M/2}^{M/2} m_{i+k,j+l}$$

By using the minimization condition

$$\frac{d\sigma^2_{ij}}{da_{ij}} = 0$$

one derives the expression

$$a_{ij} = \frac{\left\langle \left[N_{ij} - \langle N \rangle_{ij} \right] \left[n_{ij} - \langle n \rangle_{ij} \right] \right\rangle}{\left\langle \left[n_{ij} - \langle n \rangle_{ij} \right]^2 \right\rangle}$$

which defines a modulation coefficient for each point in the picture in terms of the noisy image and the idealized noise pattern. The dimension M of the local area used to determine the coefficient a_{ij} for each point is chosen on the basis of the spatial frequency bandwidth appropriate for a_{ij}.

The results of applying these techniques to remove the periodic noise component from the Mariner VII picture shown in Figure 3 are apparent in Figure 4. The complicated periodic noises which were extracted are seen in Figure 5.

Long-Line Noises - A variety of mechanisms can produce long-line or streak noises in television images such as gain variations, line bunching, data outages, and analog tape recorder drop-outs. This type of noise, caused by drop-outs in the case of Mariner 1969, becomes apparent as horizontal streaks in Figure 4 with the removal of the periodic noise. The characteristic which distinguishes streak noises from the actual scene is their linear correlation along some particular direction and the lack of correlation in the perpendicular direction. This distinction is not complete, however, since linear features are common in natural scenes. The problems of data dependent noise removal are exemplified by this case since major damage to the true video signal may result in particular localized regions which contain scene components resembling the noise.

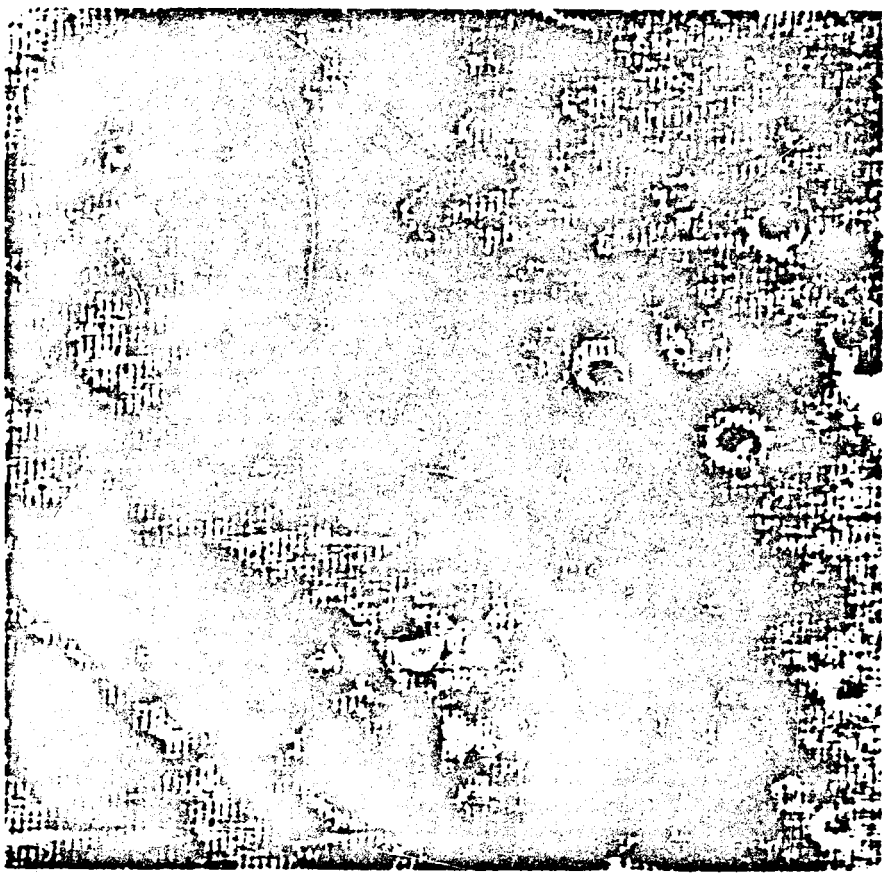

Figure 3.-A Mariner VII picture of Meridiani Sinus as received from the spacecraft and enlarged two times to make the noises apparent.

Figure 4.-The result of removing the periodic noises from Figure 3. Note the presence of horizontal streak noises at this point.

The technique developed to correct for these streak noises is to compare the local average intensity value of lines adjacent and parallel to the streaks with the average value of the streak itself and to apply a gain factor to account for any differences. A multiplicative rather than an additive correction is applied because the physical origin of the noise (magnetic tape drop-outs) is multiplicative. Since the correlation between points in a picture decreases with increasing separation, a linearly decreasing weight is applied to more distant local lines in determining the surrounding average. If N_{ij} is the noisy picture (j is the index along the direction of the streak noises) and G_{ij} is the corrective gain to be applied to the point (i,j), the expression

$$G_{ij} = \frac{\sum_{k=1}^{P} (P-k+1) \left[\langle N \rangle_{i+k,j} + \langle N \rangle_{i-k,j} \right]}{P(P+1) \langle N \rangle_{ij}}$$

is used where P is the number of adjacent lines above and below the streak and the average values are defined by

$$\langle N \rangle_{ij} = \frac{1}{Q+1} \sum_{k=-Q/2}^{Q/2} N_{i,j+k}$$

In this latter expression, Q is the low pass filter dimension along the direction of the streaks and is determined by the lengthwise correlation of the long-line noise. The dimension, P, is determined by the perpendicular correlation.

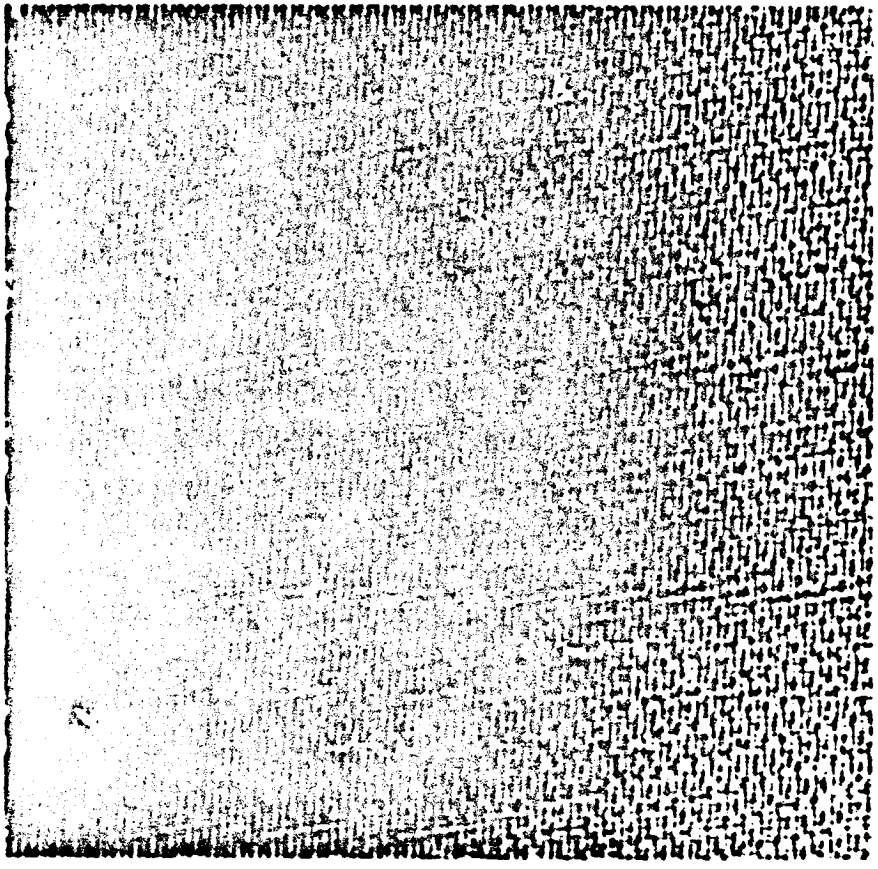

Figure 5.–The periodic noise pattern removed from Figure 3 to obtain Figure 4.

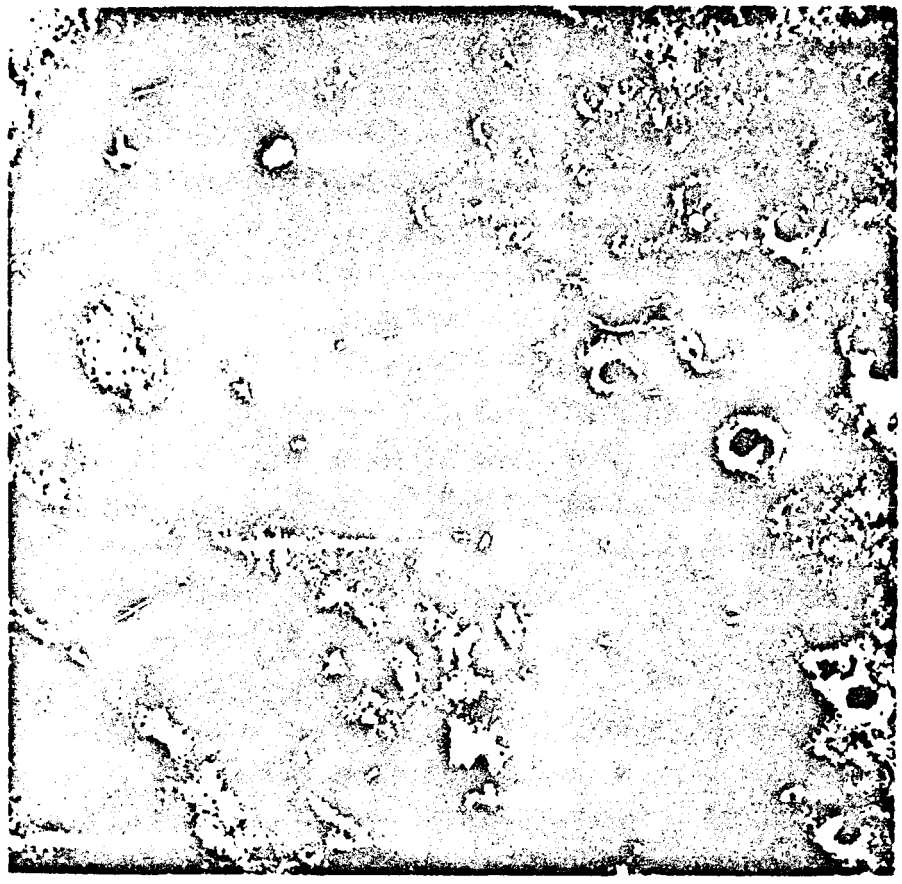

Figure 6.-The result of removing the streak noises from Figure 4. Note the presence of black and white spike noises scattered through the picture.

A further refinement was used in determining the numerator of the gain determining equation. The numerator was computed as shown but then a "majority rules" logic was applied so that terms deviating significantly from the average were eliminated from determining the average on a second pass. This algorithm is a refinement of the long-line filter described in reference 2.

The result of correcting for the streak noises in Figure 4 is shown in Figure 6. It should be emphasized that this correction is particularly data dependent and its effect, while closer to the truth in the large, may introduce artifacts in the small.

Isolated Spike Noises - The occurrence of a bit error in telemetering digital video data or the presence of sharp spikes of noise from the analog electronics can cause isolated picture elements to deviate significantly from the surrounding

data. The removal of the periodic and streak noises illustrated in Figure 6 reveals an additional noise component consisting of black and white spikes. The characteristic which distinguishes these spike noises from the actual video is the fact that because of resolution limitations of a Nyquist sampled video system the picture element to picture element variation of the true signal is limited.

The logic used to remove spike noises is very simple. Each picture element is examined and if it is significantly above each of its neighbors or significantly below its neighbors it is replaced by the average neighboring intensity. The results of applying this correction to the remaining spike noises in Figure 6 is shown in Figure 7.

A comparison of Figures 3 and 7 shows a dramatic improvement in signal-to-noise ratio by using the digital computer to isolate and remove various structured noise components from the raw video. This type of processing, while preliminary to further restorative steps, of itself produces an enhancement which allows analysis of surface detail closer to the resolution limits of the camera system. Techniques for removing noises from video are of widely varying character and in some cases strongly video system and data dependent.

Photometric Distortions

Probably the most variable and complex properties of the various types of image sensors are those affecting the conversion of light intensity to electrical signal amplitude. The discussion here centers on the photometric properties of vidicon systems but is more broadly applicable to other types of sensors. Procedures for correcting for sensitivity non-uniformity, sensitivity non-linearity, and image retentivity as a function of wavelength and temperature have been developed. In a very real sense, each encoded sample or picture element intensity value, in the output image of a camera system, can be thought of as a reading of a tiny photometer with its own unique properties. The overall properties of sensor shading, spectral response, and dynamic range, as well as local blemishes, can be considered, to a good approximation, as a composite of the corresponding properties of many such discrete independent photometers positioned at each sample point of the image.

The correction procedure which is being applied to the Mariner 1969 photographs consists of calibrating each of these photometers and then applying the appropriate linearity or residual correction to the corresponding picture element in the experiment data. The positional and geometric stability of the image raster with time is very important here since as the picture raster is displaced the correspondence between picture elements in the image and physical position on the sensor surface changes. Particularly in areas of rapid spatial variation in photometric response, such as around blemishes or reseaux, a misalignment of this type between calibration and experiment data can cause large correction errors. Calibration is achieved by exposing the sensor to a series of test targets and then extracting the absolute and relative photometric properties of each sensor element from these test images.

Residual Image - The vidicon is a good example of an image sensor exhibiting memory or residual image effects. Each output image is actually a composite of the current exposure and the retained effects of previous exposures. The residual effects of any one exposure die out in time, but the rectification of photometric distortions for a given image requires the consideration of the effects of the immediate exposure history of the sensor. In the Mariner Mars 1969 calibration a very simple model for residual image was used. The net camera output $O_j(x,y)$ for a given exposure j was assumed to be a combination of the output $E_j(x,y)$ which would result if no residual effects were present and a fraction $b(x,y)$ of the previous total camera output,

$$O_j(x,y) = E_j(x,y) + b(x,y)\ O_{j-1}(x,y)$$

Figure 7.-The result of removing the black and white spike noises from Figure 6. Note in comparison with Figure 3 that objects of considerably higher resolution are discernable in Figure 7.

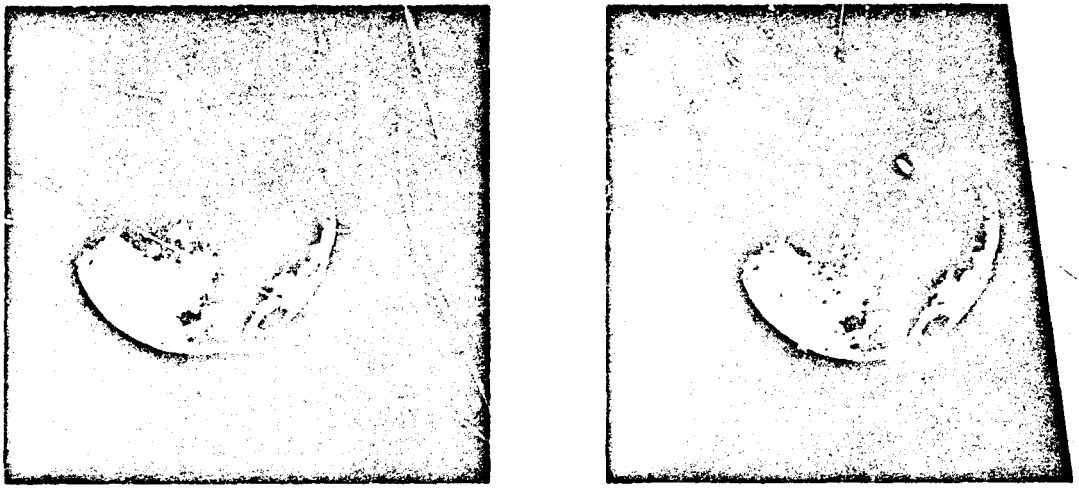

Figure 8.-The left picture is a raw photograph of the moon taken by a Mariner 1969 camera system and illustrates residual image from a prior exposure. The right picture is the result of removing the residual component by a linear combination with the previous exposure.

The residual coefficient, b, was measured as a function of position in the frame by exposing the camera to a gray wedge target constructed to produce varying gra level exposures over each local region of the sensor. The residual image coeffi· cient was then determined by reexposing the target in a slightly displaced posi- tion and measuring the remaining gray step transitions from the previous exposure In this way a residual image coefficient map was constructed as a function of position in the image format and by varying the operating conditions, as a func- tion of temperature.

An example of applying this correction procedure is shown in Figure 8. An image of the moon taken with a Mariner 1969 camera is shown in Figure 8(a) containing a residual of the previous displaced exposure. The result of applying the above correction is shown in Figure 8(b). The residual image has been removed so as not to be visible in the print but a careful investigation shows the correction to be good to only several percent. The model used is only marginally adequate and the residual coefficient exhibits strong intensity dependence. Efforts to improve the technique are under way for the Mariner Mars 1971 mission.

Photometric Linearity - Vidicon systems have limited dynamic ranges and exhibit light transfer curves relating the camera output to input luminance level, simi- lar to H & D curves for film systems. Because of various mechanisms causing non- uniform sensitivity in the tubes (oblique beam landing and blemishes), each point in the tube exhibits a unique light transfer curve. Appropriate curves are generated simultaneously for each point by sequentially exposing the camera to spa- tially uniform illuminations with varying intensities. Wavelength and tempera-

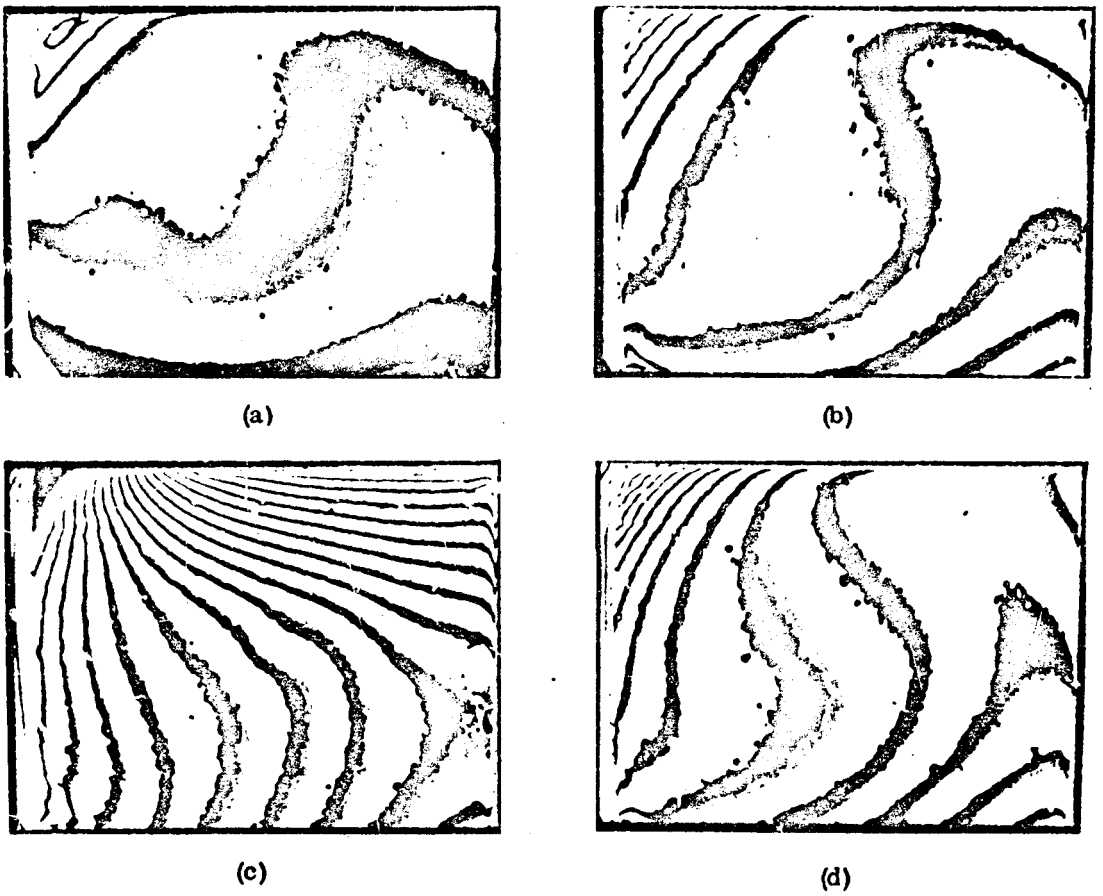

Figure 9.-A sequence of contoured flat field calibration frames from a Mariner 1969 camera system. Contouring was achieved by suppressing the five most significant bits of eight prior to display. The light levels are (a) 100 Foot-Lamberts, (b) 400 Foot-Lamberts, (c) 800 Foot-Lamberts, and (d) 1600 Foot-Lamberts.

ture dependence is determined by altering the spectral filtering of the light source and the operating temperature. The light transfer curve for each point in the image is stored on magnetic tape and is applied to correct the corresponding element in the actual experiment data. A sufficient number of points on each curve is measured to guarantee that a linearly interpolated correction produces adequate accuracy.

Contoured examples of four such flat field exposures are shown in Figures 9(a) through 9(d). The contours were generated by removing the five most significant bits from the eight bit calibration data thereby producing a "saw tooth" effect in the image display. The changing shapes of the contours with changing light levels is apparent and indicates a strong spatial dependence of the sensor light transfer properties. The presence of isolated blemishes and reseaux is also apparent.

Geometric Distortions

Geometric distortions in the output of an electronic imaging system arise in many ways and must be removed in order to measure the geometric shapes and relationships between objects in the scene, as well as to properly align calibration data with experiment data. This latter consideration is important, for example, in the alignment of photometric sensitivity data taken prior to flight with the data returned by a space mission, since a raster shift is typical once the device is removed from the earth's magnetic field. In Mariner class systems, shifts of the order of five to ten picture elements are common. In addition, small shifts from frame to frame due to electronic sweep variations can also occur.

The major sources of distortion in vidicon systems, apart from foreshortening due to oblique photography, are optical distortions, electronic raster sweep distortions, and raster shifts due to changes in the magnetic environment. A negligible effect in vidicon systems is mentioned only because it is important in other types of sensors and represents an interesting problem. This effect is called "beam bending" and arises because as the sensor charge image is read out and discharged small tangential electric fields are set up on the tube target which are a function of the recorded image intensity. These fields can cause a corresponding displacement of the readout electron beam, particularly for low energy electrons, and introduce an image dependent geometric distortion.

For the Mariner television experiment, the optical and electronic geometric distortions are characterized by measuring separately the overall system distortions and the frame to frame electronic distortion fluctuations. The system distortions are determined by measuring the relative displacements of the intersections of a precise grid target after being photographed by the system. The electronic distortions are determined by measuring the relative displacements of the images of reseaux in a pattern permanently deposited on the sensor tube target. This reseau pattern allows the frame to frame tracking of electronic changes. The corresponding stability problem in the case of optical distortions does not exist typically.

The correction for geometric distortions is then performed in two steps. Since the reseau pattern is permanently affixed to the tube and since the reseaux must not obscure a sizable portion of the image area, they are typically too sparse to determine, in detail, the electronic geometric distortions. The frame to frame electronic shifts as well as the shifts due to magnetic environment changes are, however, typically small and are largely simple translations in the raster. Thus, the reseaux are used to apply a small and largely homogeneous correction on a per frame basis to align the reseaux of a particular frame with those in the calibration grid target frame. The more detailed and precise system distortion correction is then applied to the result. Partially successful attempts have been made to automate, in the computer, the reseau detection and measurement procedure, on a per frame basis, to accommodate the overall correction process.

The actual application of the geometric distortion correction to the raw sampled output of the camera is conceptually the superposition of a new, non-uniform set of sample points on the raw data. The positions and local spacings of the new sample points are determined by linearly interpolating the distortion data derived

from the calibration frames. Clearly the locations of the new sample points will not be commensurate with the uniform sampling of the raw camera output so that interpolation of the intensity data is required to determine the intensity values at the new sample locations. If the raw image was not Nyquist sampled, this interpolation process can severely degrade the corrected image resolution.

The result of photographing a grid target with a Mariner 1969 camera is shown in Figure 10(a). A significant pin-cushion distortion is evident. The result of applying the above correction is shown in Figure 10(b). The location corrections for points between the various grid target intersections were determined by linear interpolation.

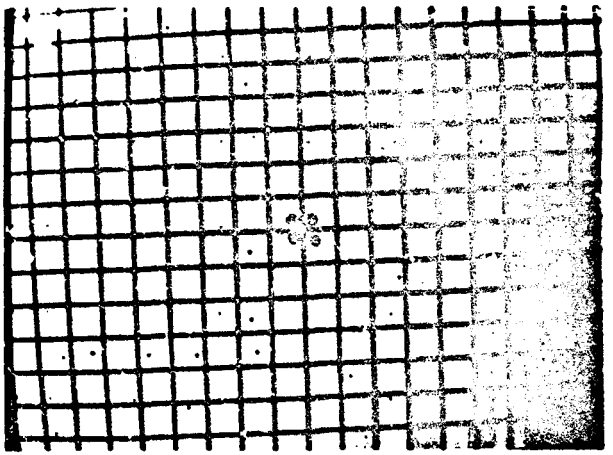

(a)

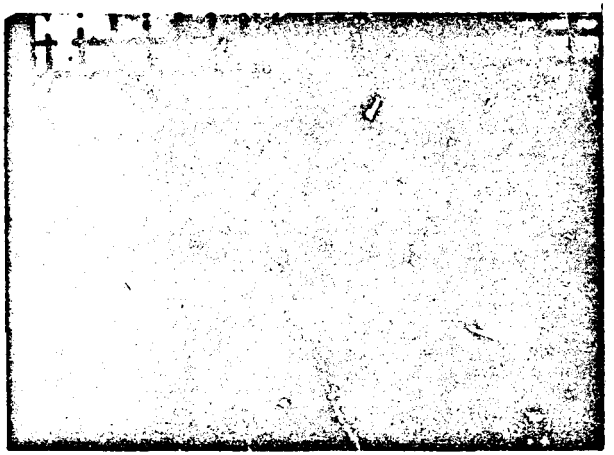

(b)

Figure 10.-Grid patterns. (a) Grid pattern photographed through a Mariner 1969 camera system exhibiting barrel distortion. (b) Result of computer correction of the distorted target.

Resolution Enhancement

The scale size of object scene detail visible through a television camera is limited, in a perfect system, by diffraction effects in the optics. This, of course, ignores the effects of atmospheric turbulence. For most systems this limit is not realized as the camera sensor system itself imposes resolution limitations which are dominant. In any case, the result is an apparent loss of contrast in small scene detail (small relative to the resolution of the system) or equivalently a broadening of the transitions between adjacent intensities in the camera output. These effects influence not only the visibility of scene detail for photointerpretive purposes but also photometric measurement accuracy on small detail.

If the camera system is linear or if the input scene is sufficiently low in contrast, the degradation in image resolution is describable in terms of an amplitude independent system point spread function. If the point spread function is furthermore independent of position in the image plane, such as for narrow angle systems, then the camera output, $O(x,y)$, can be written in terms of the object scene intensity distribution, $I(x,y)$, and the system point spread function, $S(x,y)$, by a simple convolution relation

$$O(x,y) = \int du \int dv \;\; I(x+u,y+v)\; S(u,v)$$

This relation can be inverted using Fourier transformations to express the desired input scene in terms of the camera output

$$I(x,y) = \int du \int dv \;\; O(x+u,y+v)\; F(u,v)$$

$F(x,y)$ is a correction filter related to the point spread function through the relation

$$F(x,y) = \mathcal{F}^{-1}\left[\frac{1}{\mathcal{F}\left[S(x,y)\right]^*}\right]$$

where $\mathcal{F}[\;]$ is the Fourier transform operator.

This sequence of equations has a discrete counterpart appropriate to digital computation. The additional condition of Nyquist sampling must be imposed in the discrete case for validity.

The correction filter function F is a function only of the uniform camera point spread function and thus may be calibrated independently of the object scene. This is done for the Mariner 1969 experiment by measuring the modulation transfer

function (MTF) or the Fourier transform of the point spread function rather than the point spread function directly. The reason is that for vidicon systems, in order to produce a sufficient output point spread amplitude to make reliable measurements for all spatial frequencies, the input must be so large as to drive the system into non-linear response. The MTF is measured by exposing the camera to spatial sine wave transmittance targets of various frequencies and orientations and extracting the sine wave amplitude degradation along the line scan and perpendicular to the line scan directions. These curves are then used to model the two-dimensional MTF function by assuming the contours of equal response are ellipses. The phase component of the MTF is ignored, not so much as justified as because the measurement of phase properties has not been possible. The resulting MTF is then used to generate the correction filter.

The correction filter is theoretically the reciprocal of the MTF function. For typical systems however, the response at high spatial frequencies becomes quite low so that gains in excess of ten at these frequencies are necessary. The addition of wideband noises within the system make this theoretical correction undesirable. Since the scene spectral components decrease in amplitude at high frequencies and add coherently and since the noise is essentially white and adds incoherently, any filter correction degrades the gross signal-to-noise ratio of the resulting image. Thus some criterion for suppressing the large high spatial frequency gains is necessary based on the competition between small feature and edge transition fidelity and degraded signal-to-noise ratio.

There are quantitative criteria for this trade-off and correction filter generation such as the Wiener-Hopf filtering technique. For many purposes, however, these are unacceptable since they are based on large scale statistical measures of error and in the small, produce less than optimum results. Adaptive filtering approaches, based on both large scale and small scale fidelity, are most desirable but are expensive in terms of computer time. Continued development in this area is under way.

For many purposes a simple trial and error solution to the problem is adequate. In Figure 11 a typical MTF curve is shown and labelled A . The theoretical correction filter based on this MTF is shown as curve B . By introducing an artificial truncation to the theoretical curve, such as shown in the dashed curves labelled C , the emphasis of high spatial frequency noise amplification can be controlled. A filter or series of filters consistent with the camera signal-to-noise properties, the typical scene spectral composition, and experiment measurement goals can be derived.

Examples of applying this type of truncated MTF correction to a Mariner Mars 1971 test scene are shown in Figures 12 through 14. The raw camera output is shown in Figure 12 and the results of resolution enhancements with gain truncations at 2.5 and 10.0 respectively, are shown in Figures 13 and 14. A comparison of these results show the most subjective improvement between Figure 12 and 13 with a slight additional sharpening in Figure 14 but a more significant increase in noise levels.

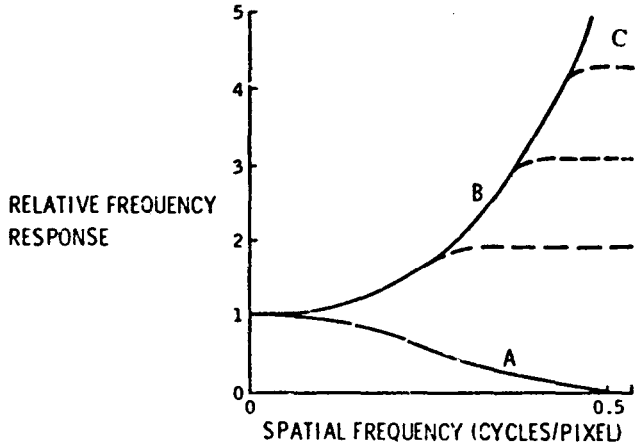

Figure 11.- Modulation transfer function and correction filter spectra. Curve A shows a typical modulation transfer function (MTF) for a vidicon system. Curve B shows the theoretical reciprocal correction filter function. Curves C (dashed) show various gain truncations of the theoretical correction curve used to minimize the signal-to-noise degradation caused by the enhancement process.

Figure 12.-Raw output image of a Mariner Mars 1971 breadboard television camera An Apollo 11 photograph of the moon was used as the test target.

Figure 13.- High spatial frequency enhanced version of Figure 12 with a gain truncation of the correction filter spectrum at 2.5.

Figure 14.- High spatial frequency enhanced version of Figure 12 with a gain truncation of the correction filter spectrum at 10.0.

These corrections were applied as convolution filters with the kernels generated from the reciprocal MTF function rather than as direct frequency space filters. The reason is strictly one of economy. The convolution kernel matrix for these corrections needs be only on the order of 15 picture elements square and increased calculation speed is realized by matrix convolution rather than transformation. This trade-off is, of course, machine dependent. An example of the opposite trade-off is that of the previously discussed periodic noise filtering. In order to obtain sufficiently narrow frequency space bandpass characteristics, the convolution kernel would be prohibitively large thereby making direct transform space filtering the more economical approach.

Conclusion

The inherent physical limitations in camera system and sensor capabilities introduce significant distortions into the imagery which is recorded. Careful measurements on such imagery must take these effects into account. The digital computer is an extremely useful tool for this purpose offering precision and flexibility to solve non-linear as well as linear distortion problems in a highly controlled and reproducible manner. Techniques have been demonstrated and continue to be improved for the correction of camera system noise, photometric, geometric and resolution distortions. The application of digital image processing techniques makes possible quantitative scientific investigations using television imagery which would not be possible otherwise.

ACKNOWLEDGMENT

This work is the result of the collective contributions of many people, in addition to the author, in the areas of algorithm design, software development and applications, and hardware system development. Principally these people include F. Billingsley, R. Brandt, Dr. J. Dunne, H. Frieden, E. Johnson, Dr. R. Nathan, and W. Stromberg.

REFERENCES

1. Billingsley, F.C., "A Digital Image Processing Rationale," Journal of the Association for the Advancement of Medical Instrumentation, Vol. 3, No. 1, January 1969.

2. Nathan, R., "Digital Video-Data Handling," JPL TR 32-877, January 5, 1966.